

Experimental Study of Pressure Drop and Wall Shear Stress Characteristics of γ /Al₂O₃-Water Nanofluid in a Circular pipe under Turbulent flow induced vibration.

Adil Abbas AL-Moosawy

Hatem H. Obeid

Hameed K. Hamzah

Department of Mechanical Engineering, Babylon University, Iraq.

Hameedkadhemi1977 @Gmail.com

Abstract

Experimental study of γ /Al₂O₃ with mean diameter of less than 50 nm was dispersed in the distilled water that flows through a pipe consist of five sections as work station ,four sections made of carbon steel metal and one sections made of Pyrex glass pipe, with five nanoparticles volume concentrations of 0%,0.1%,0.2%,0.3%,and 0.4% with seven different volume flow rates 100, 200 , 300, 400, 500, 600 ,and 700ℓ/min were investigated to calculated pressure distribution for the cases without rubber ,with 3mm rubber and with 6mm rubber used to support the pipe. Reynolds number was between 20000 and 130000. Frequency value through pipe was measured for all stations of pipe for all cases. The results show that the pressure drop and wall shear stress of the nanofluid increase by increasing the nanoparticles volume concentrations or Reynolds number, the values of frequency through the pipe increase continuously when wall shear stress increases and the ratio of increment increases as nanofluid concentrations increase. Increasing of vibration frequency lead to increasing the friction factor between the pipe and the wall and thus increasing in pressure drop. Several equations between the wall shear stress and frequency for all volume concentration and for three cases without rubber, with rubber has 3mm thickness ,and with rubber has 6mm thickness. Finally, the results led to that γ /Al₂O₃ could function as a good and alternative conventional working fluid in heat transfer applications. A good agreement is seen between the experimental and those available in the literature.

Keywords: Experimental study; γ / AL₂O₃ nanofluid ; Turbulent flow ; Flow induced vibration ; Pressure drop, wall shear stress.

الخلاصة

في هذا العمل أجريت دراسة عملية لمائع نانوي متكون من جزيئات اوكسيد الألمنيوم نوع كما ذات معدل قطر اقل من (50 nm) ثم تعليقها في ماء مقطر بخمسة تراكيز حجميه مختلفة يتدفق المائع النانوي عبر أنبوب مصنوع من الصلب الكربوني بسبعة معدلات جريان حجميه مختلفة في منطقة الجريان الاضطرابي. تم حساب توزيع الضغط عبر الأنبوب في ستة مقاطع عمليا وكذلك التردد الاهتزازي للأنبوب وثلاث حالات بوجود مادة مطاطية لإسناد الأنبوب سمك ٦ ملم وسمك ٣ ملم وحالة أخرى بدون استخدام مادة مطاطية . المادة المطاطية استخدمت لتقليل الاهتزاز الناتج من جريان المائع النانوي .أوجدت النتائج بان قيم انخفاض الضغط وإجهاد القص تزداد بزيادة التركيز ومعدلات الجريان اي بزيادة رقم رينولد. كذلك زيادة إجهاد الاهتزاز يؤدي إلى زيادة إجهاد القص وبالتالي زيادة انخفاض الضغط. تم إيجاد مجموعة معادلات تجريبية بين تردد الأنبوب وإجهاد القص الناتج من الجريان ولكافة الحالات التي تم دراستها. وكذلك تم الحصول على توافق بالنتائج مع البحوث السابقة لقيم الضغط والاهتزاز.

الكلمات المفتاحية: دراسة تجريبية؛ γ / AL₂O₃ nanofluid ؛ الجريان المضطرب ؛ تدفق الاهتزاز الناجم . انخفاض الضغط ، والإجهاد جدار القص .

1.Introduction

The analysis performed on experimental laboratory data provides the main source of information about nanofluid flow regimes. This study describes the experimental part of the present work which include design and build up the experimental rig , that can be used to study evaluating the pressure distribution, and pressure drop at different Reynolds number in horizontal circular pipe with different concentrations of nanofluid. Also, evaluating velocity along stages of pipe with different concentration of nanofluid ,and flow rate. Kohli and Nakra [1984] carried out a simplified finite element analysis in which straight beam finite elements was used in order to determine the natural frequencies of vibrations of straight and curved tubes conveying fluid at a constant velocity. Results compared with as analytical method with three elements and gave good agreement between the results.

Paidoussis and Issid [1994] studied dynamics and stability of flexible pipes containing flowing fluid, where the flow velocity is either entirely constant, or with a small harmonic component superposed. An extensive historical review of the subject is given. In the case of constant flow velocity, the dynamics of the system is examined in a general way and it is shown that conservative systems are subject not only to buckling (divergence) at sufficiently high flow velocities, but also to oscillatory instabilities (flutter) at higher flow velocities. Also presented are some new results for cases of systems subjected to internal dissipative forces. In the case of harmonically varying flow velocity, the equation, of motion derived here exposes an error in a previous derivation. Stability, maps are presented for parametric instabilities,. It is found that the extent of the instability regions increases with flow velocity for clamped-clamped and pinned-pinned pipes, while a more complex behaviour obtains in the case of cantilevered pipes. In all cases, dissipation reduces the extent of, or entirely eliminates, parametric instability zones. **Chang and Chiou [1995]** studied the natural frequencies and critical velocities of laminated circular cylindrical shells with fixed-fixed ends conveying fluid by Equations of motion were derived by the Hamilton principle under the scope of Mindlin-type first order transverse shear deformable cylindrical shell theory. Dynamic characteristics equations were then obtained under the assumption of harmonic motion, and the natural frequencies corresponding to each flow velocity were found. Numerical examples were presented, which, include stacking angle. **Lin and Tsai [1997]** studied a finite element approach for nonlinear vibration analysis of Timoshenko pipes conveying fluid. An approach using the concept of fictitious loads to account for the kinematic corrections was applied to establish the finite element model, without the need to solve the nonlinear equations of motion. Computation of system responses was carried out by iteratively updating the nodal coordinates until convergence was reached. The formulation and implementation of the approach were verified first by comparing the analysis results with those available in the literature for the case of both slender and short beams undergoing static large deformations and the case of flow induced vibration of a slender cantilever pipe with supercritical flow speeds. Limit cycle and its associated vibration amplitude for the flow induced vibration problem were discussed. Further analysis was conducted for assessment of the effects of flow speed and fluid/pipe mass ratio on the limit cycle vibration amplitude. The influence of slenderness ratio on the limit cycle amplitude was also reported. **Willatzen [2003]** examined the influence of a moving fluid confined by a solid circular cylindrical shell on the propagation of acoustic waves generated by sources located on the circular cylindrical shell. An expression for the acoustic pressure in a moving fluid is derived including azimuthally asymmetry effects in the general case, where the fluid velocity points along the cylindrical shell axis and can be written as an infinite power series expansion in the radial co-ordinate. Secondly, continuity of pressure and normal velocity at the liquid-shell interface is imposed to derive a set of coupled differential equations governing the possible vibration modes of the shell and determine dispersion relations, i.e., mode propagation constants β as a function of frequency as well as changes in β values accommodated by flow. In the remaining part of the paper, phase speed changes with flow and transit-time differentials of circular cylindrical shell vibrations are discussed with special emphasis to flow measurement properties. **Pittard et. al.[2004]** studied flow-induced pipe vibration caused by fully developed pipe flow has been observed but not fully investigated when take place turbulent flow. studied experimental results that indicate a strong correlation between the volume flow rate and a measure of the pipe vibration. In this work, the standard

deviation of the frequency-averaged time-series signal, measured using an accelerometer attached to the pipe, is used as the measure of pipe vibration. The results from the numerical LES models also indicate a strong correlation between pipe vibration and flow rate. In general, the numerical simulations show that the standard deviation of the pipe wall vibration is proportional to the pressure fluctuations at the wall induced by the flow turbulence. This research, indicates that the pressure fluctuations on the pipe wall have a near quadratic relationship with the flow rate. Furthermore, the experimental results and the numerical modeling show that there is a definite relationship between the acceleration of the pipe (pipe vibration) and the flow rate. **Birgersson et. al. [2004]**, studied the vibration of pipes using the Arnold–Warburton theory for thin shells and a simplified theory valid in a lower frequency regime. The vibration response is described numerically with the spectral finite element method (SFEM), which uses the exact solutions of the equations of motion as basic functions. For turbulence excitation, the set of basic functions was extended to include particular solutions, which model a spatially distributed excitation. An efficient numerical solution to homogeneous random excitation is presented and the results compare favorably with wind tunnel measurements. **Jeong et. al. (2006)** studied the vibration analysis and dynamic behavior of a thin-walled shell was based on Sander’s theory, and the fluid was considered as inviscid and incompressible, so that it satisfies the Laplace’s equation. An estimation of frequency response function of the pipe considering the coupled effects of the internal fluid was presented. The influence of fluid velocity on the frequency response function was illustrated and discussed, and the results by this method were compared with published results. **Bagchi et. al. [2009]** studied experimentally the effect of pipe oscillations on the wall pressure field and flow rate through a metallic pipe with air flowing through it. The data presented in this study showed that the frequencies of pressure oscillations in a non-oscillating pipe were identical to the natural structural modes of the pipe suggesting the influence of structural properties on the fluid dynamics of the flow. The results showed that the wall pressure undergoes both a temporal as well as a spatial oscillation if the pipe was forced to oscillate periodically. The flow rate through the pipe was seen to undergo a periodic change over a range of almost 7 percent variation when the pipe was oscillated. **Wang and Dai [2012]** investigated the vibration and stability properties of fluid-conveying pipes with two symmetric elbows fitted at downstream end. The fluid, after entering from the upstream end, is pushed downwards and eventually exits from the downstream end fitted with two symmetric elbows. The equation of motion is solved by means of Galerkin’s method with a four-mode approximation. Calculations are conducted for cantilevered and also for pinned–pinned slender pipes. Result is found that the stability of the pipe system can be greatly enhanced with such downstream elbows. The vibration frequency of the fluid-conveying pipes can be comfortably controlled due to the downstream elbows with a selection of angle of inclination. The proposed geometry configuration of fluid-conveying pipes may be useful for the design and improvement of engineering pipeline systems and fluidic devices. **Adelaja [2013]** investigated the nonlinear transverse vibration of a flexible pipe conveying hot, pressurized fluid. The pipe which is subjected to a pinned-pinned end condition extends as a result of several operating variables such as internal fluid temperature variation, pre-stress and internal pressurization. The equation of motion is solved analytically by hybrid

Fourier-Laplace transforms, and the effects of inlet temperature, temperature gradient, and coefficient of area deformation are investigated on the natural frequencies and transverse dynamic response of the pipeline. **Sahib[2013]** Studied numerically, analytically and experimentally the fluid flow and pipe structure, and coupled by the forces exerted on the structure by fluid. The effect of design parameters such as pipe diameter, pipe wall thickness, pipe material and the effect of fluid velocity on the flow-induced vibration (FIV), natural frequency and damping ratio of a straight pipe conveying fully developed turbulent flow Also investigated the effect of support conditions (simply- simply and clamped- clamped) Mathematically, the governing continuity and momentum equations with a standard (k- ϵ) turbulence model associated with laws of the wall along solid boundaries are solved numerically Experimentally, the work is carried out on a build up rig. Pipe vibrations were characterized by accelerometer mounted on the pipe wall The experimental and theoretical results show that the pipe vibration level specify dependence on design parameters does not appear to be constant with flow rate, with pipe vibration level becoming less dependent on design parameters with decreasing flow rate, as well as the effect of these parameters are greater in the clamped-clamped condition.

From the literature can be concluded that most of the works focused on the mechanisms of instability of vibration and dynamic of pipes conveying fluid by using analytical method such as, Galerkin method, and some of researches focused on the effect of added external force on flow field structure in pipe conveying fluid or studied the effect of external vibration on laminar flow by putting obstacle such as orifice or studied pulsating flow. It is obvious from the literature review; a little attention was made for the effect of turbulent flow on the dynamic behavior of a pipe conveying fluid. Therefore, this work involves experimental studies for effect of fully developed turbulent flow of $\gamma/\text{Al}_2\text{O}_3$ nanofluid to find relation between frequency of pipe and wall shear stress. Also calculate the vibration shear stress as a function volume concentration and Reynolds number.

2.Experimental Apparatus and Procedure.

A schematic of the experimental setup shown in Fig. 1, used to measure pressure at six locations in pipe for various flow rates . It includes a pump, test section, Pyrex glass section, reservoir. The working fluid was pumped using positive displacement gear pump was chosen to deliver the fluid system ,i.e. the pump Gool Pompetravaini type (PMPA TIPO). The motor was ASINCRONG-IEC type (FELM), 3-Ph and 1500 r.p.m .It has a maximum capacity of 13m³/hr. The test section consisted of a circular carbon steel pipe of 80 mm inner diameter and 82mm outer diameter with 6m length. The pipe was divided to five sections, four of carbon steel with a length of 1m and one section of Pyrex glass pipe has a length of 2 m. The two ends of the test section are connected to the rest of circulatory system by using plastic flanges. The water reservoir has a capacity of 500 liters, with dimensions 1m x1m x 0.5m. Six pressure sensors were used to measure the pressure along the test section. The pressure sensor was calibrated by measuring the pressure by manometer at each point of sections of pipe and used to correct the pressure reading. After passing through the test section, the flow rate was measured by a standard flow meter type (F.M 914232) .The actual flow rate range from 100 ℓ /min to 700 ℓ /min. The liquid flow meter was calibrated by measuring the actual flow rate using stopwatch and volumetric flask at each point of interest allowing calibration curve being represented. The experimental repeated for three cases without rubber, with rubber

has 3mm thickness and with rubber has 6mm thickness. The frequency of pipe measured by using Sound and Vibration Data Acquisition (NI USB-4431). Fig.2 represented a photograph of a schematic diagram of the experimental set up .

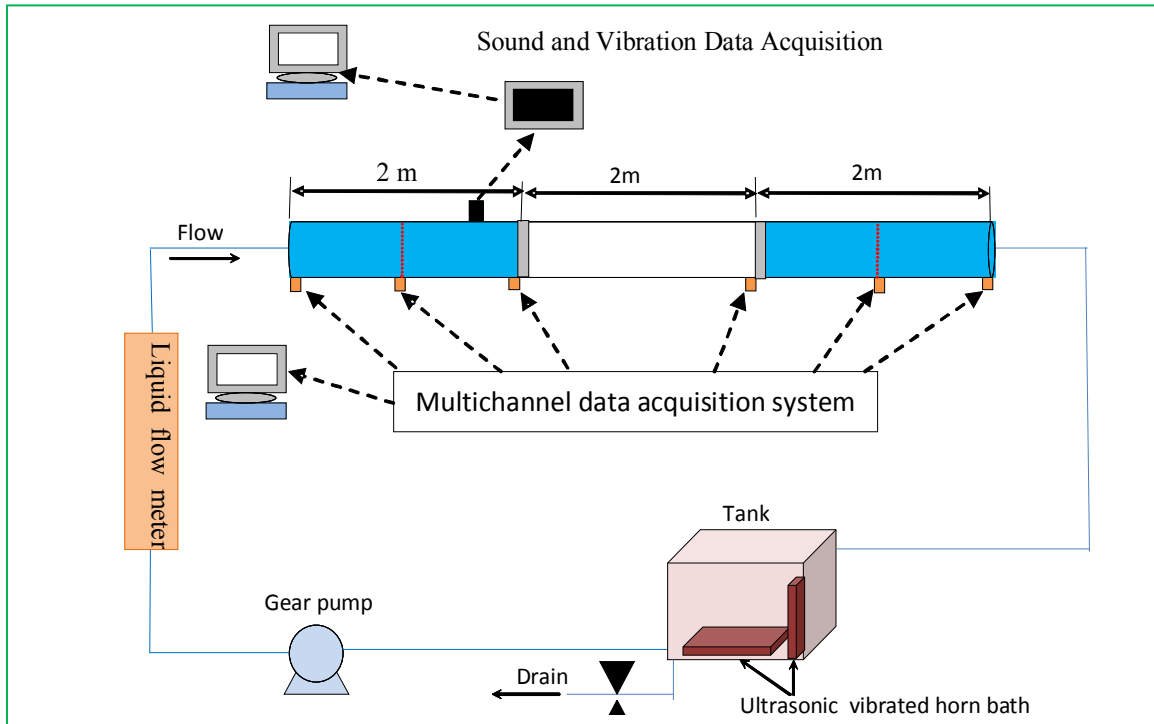


Fig. (1) schematic diagram of the experimental set up.

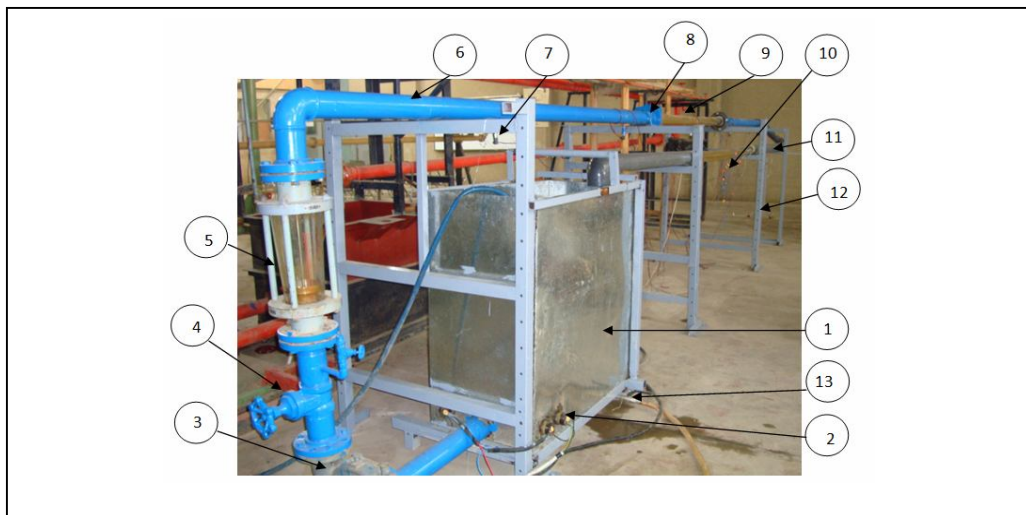


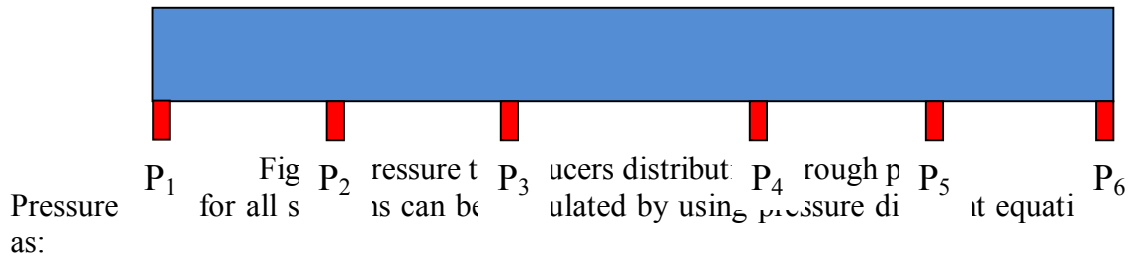
Fig. (2) photograph of a schematic diagram of the experimental set up.

1. Fluid reservoir
2. Heater
3. Gear pump
4. Valve
5. Liquid flow meter
6. Circular pipe of Carbon steel
7. Pressure sensor
8. Clamped stud
9. Pyrex glass pipe
10. Thermocouple
11. PVC pipe
12. Stud
13. Drain

3. Experimental calculation

3.1. Pressure Drop Calculation

The pressure across the test section was measured by using pressure transducer as shown in figure 3 .



$$\begin{cases} \Delta p_1 = P_2 - P_1 \\ \Delta p_2 = P_3 - P_2 \\ \Delta p_3 = P_4 - P_3 \\ \Delta p_4 = P_5 - P_4 \\ \Delta p_5 = P_6 - P_5 \end{cases} \quad \dots (1)$$

3.2. Shear Stress and Reynolds number Calculation.

The mean shear stress ,at the wall of nanofluid and of all flow regimes is given by Raja, et al. [2012] as:

$$\tau_{wall} = \left(\frac{\Delta P}{\Delta z} \right) \left(\frac{D}{4} \right) \quad \dots (2)$$

And, Reynolds number is given by Holmen [2010]

$$Re_{nf} = \frac{\rho_{nf} u_{nf} D}{\mu_{nf}} \quad \dots (3)$$

3.3. Frequency measurement

Frequency describes the number of waves that pass a fixed place in a given amount of time. So if the time it takes for a wave to pass is 1/2 second, the frequency is 2 per second. If it takes 1/100 of an hour, the frequency is 100 per hour. Usually frequency is measured in the hertz unit. The frequency of the pipe can be experimentally measured by oscilloscope for each cases with and without rubber at different flow rate . The experimental results include the calculation of the frequency of pipe (f_d) without fluid flow and frequency of pipe (f_w) with nanofluid flow ,the value of (f_w) change with flow rate and if this value is equal to nature frequency this led to resonance phenomenon. The values of (f_w) and (f_d) are drawn with Reynolds number to determination the resonance phenomenon avoid it .

3.4. Calculation Mass of Pipe with Nanofluid .

Mass of pipe with nanofluid represent mass of pipe material and mass of nanofluid inside the pipe as shown in figure 4.

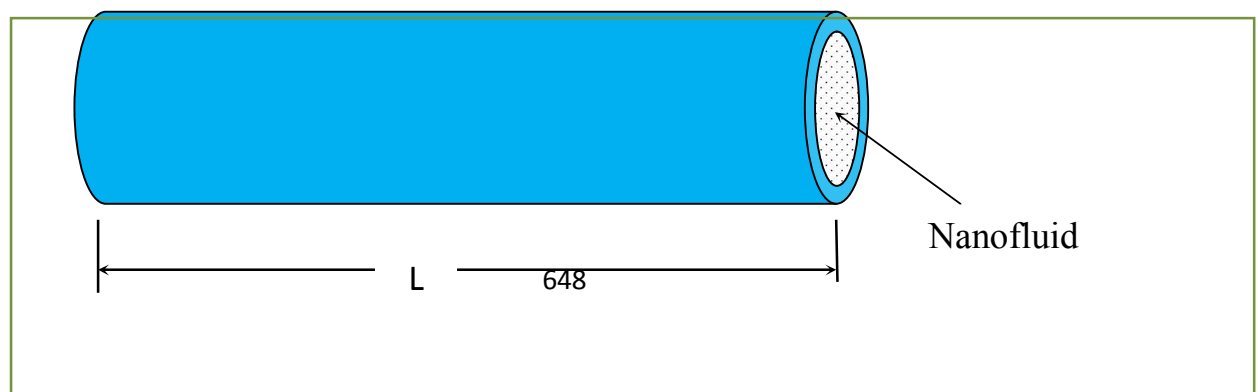


Fig. (4) section of pipe filled with nanofluid.

$$m_p = \rho_p \times v_p \tag{4}$$

$$v_p = \frac{\pi}{4} \times (d_o^2 - d_i^2) \times L \tag{5}$$

$$m_{nf} = \rho_{nf} \times v_{nf} \tag{6}$$

$$v_{nf} = \frac{\pi}{4} \times d_i^2 \times L \tag{7}$$

$$m = m_p + m_{nf} = \left[\rho_p \times (d_o^2 - d_i^2) + \rho_{nf} \times d_i^2 \right] \times \frac{\pi}{4} \times L \tag{8}$$

ρ_{\neq} is represent ρ_{\neq} for stations 1,2,4 ,and 5 ,while $\rho_{p\neq}$ is represent for station 3.

Table.1 calculation of mass pipe filled nanofluid with station .

| Stations No. | Mass of nanofluid (kg) | | | | |
|--------------|------------------------|----------|----------|----------|----------|
| | 0 % | 0.1 % | 0.2 % | 0.3 % | 0.4 % |
| 1 | 6.923955 | 7.143504 | 7.294224 | 7.444944 | 7.59064 |
| 2 | 6.923955 | 7.143504 | 7.294224 | 7.444944 | 7.59064 |
| 3 | 11.01456 | 11.45365 | 11.75509 | 12.05653 | 12.34793 |
| 4 | 6.923955 | 7.143504 | 7.294224 | 7.444944 | 7.59064 |
| 5 | 6.923955 | 7.143504 | 7.294224 | 7.444944 | 7.59064 |

3.5. Calculation Vibration Shear Stress .

The shear stress which was generated pipe vibration was calculated with flow rate and concentration of nanofluid flow with and without rubber for all sections of pipe. according to Blevins [1977].

$$P_0 = F \times V_a \tag{9}$$

$$P_0 = m \times A_a \times V_a \tag{10}$$

$$\tau_{vib} \times V = m \times A_a \times V_a \tag{11}$$

$$\tau_{vib} = \frac{m \times A_a \times V_a}{V} \tag{12}$$

Where : P_{\neq} is the power, A_{\neq} is the actual acceleration of pipe, and V_{\neq} is the actual velocity of pipe. τ_{vib} vibration stress generated by vibrated pipe, mass of pipe with nanofluid.

3.6. Calculated damping ratio.

The damping ratio can be calculated for three cases of pipe without rubber ,and with rubber has thickness 3 mm ,and with rubber has thickness 3 mm. The calculation of damping ratio depend on the amplitude of two successive peaks in amplitude time curve for case 0.4 % Al_2O_3 and 600 l/min flow rate as shown in figures (5),(6),and (7). The values of amplitude calculated with time by using software NI signal express 2015 used to analysis the results from sound and vibration assistant. The damping ratio relation with amplitude according to Francis [1983].

$$\zeta = \frac{1}{\sqrt{1 + \left[\frac{\pi}{\ln\left(\frac{y_1}{y_2}\right)} \right]^2}} \quad \dots(12)$$

where

ζ is the damping ratio ,and y_1 , and y_2 are the amplitude of two successive peaks.

The damping ratio is calculated according to above equation for case 0.4 % Al_2O_3 and 600 l/min flow rate as: ζ for tow rubber case is 0.15 ,and 0.21 for one rubber case ,and 0.254 for without rubber case. Figures 5 ,6,and 7 represent the experimentally relation between amplitude and time for three cases of support with 6mm rubber, 3mm rubber , and without rubber.

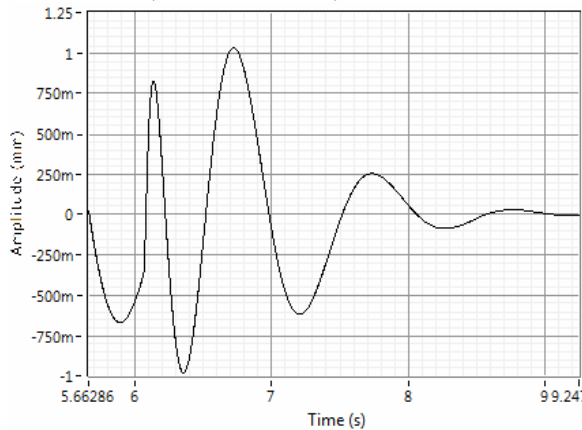


Fig. 5 relation between amplitude and time for pipe with two rubber

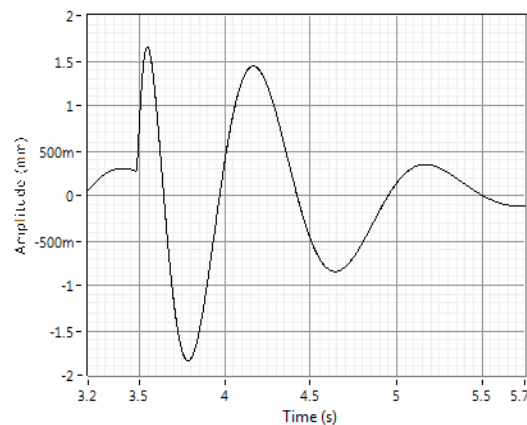


Fig. 6 relation between amplitude and time for pipe with one rubber

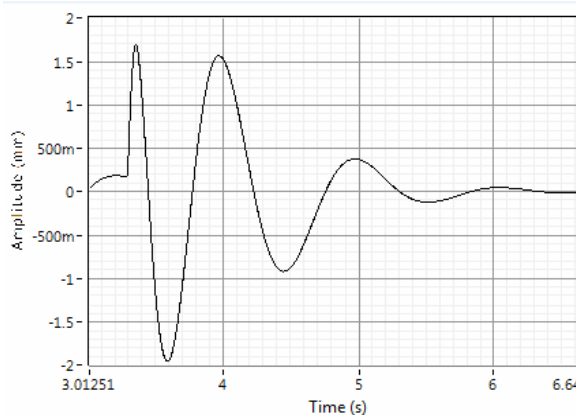


Fig. 7 relation between amplitude and time for pipe without rubber

4. Thermo-physical Properties of Nanofluid.

The transport properties such as density of nanofluids ,the density was calculated by using the mean fluid temperature between the inlet and outlet. The physical properties of the nanofluid that are taken as function of the volume concentrations, are defined as follows:

1. Density

The effective density of the nanofluids containing suspended particles can be evaluated by the following equation :

$$\rho_{nf} = (1 - \varphi)\rho_{bf} + \varphi\rho_p \quad \dots(14)$$

The above equation has been experimentally validated by Pak and Cho [1998].The viscosity of the nanofluid was illustrated by Raja, [2012] is defined as follows:

$$\mu_{nf} = \mu_{bf}(1 + 2.5\phi) \quad \dots(15)$$

Tables (2),and (3) describe the property (density)of Al₂O₃/γ nanoparticle and base fluid .

Table .2 density of Al₂O₃/γ nanoparticle and base fluid . Holman [2010]

| Temperature (°C) | 40 | 50 | 60 |
|-----------------------------------|------|-------|-------|
| Al ₂ O ₃ /γ | 3970 | 3970 | 3970 |
| Pure water | 993 | 988.8 | 983.3 |

Table.3 calculation of the density of nanofluid at temperature 60 °C.

| φ(%) | 0 | 0.1 | 0.2 | 0.3 | 0.4 |
|--------------------------------------|----------|---------|---------|---------|---------|
| ρ _{nf} (kg/m ³) | 983.3 | 1027 | 1057 | 1087 | 1116 |
| (kg/m.s) | 0.000949 | 0.00102 | 0.00113 | 0.00162 | 0.00141 |

4. Preparation of Nanofluid

The following procedure represents the steps that has been used in the present work to make the required preparation of the nanofluid. Weighting the powder required for each concentration by a sensitive balance , and adding the weighted nanoparticles to five liters of the distilled water, reported by Fotukian *et. al.*[2010]:

$$\phi \% = \frac{(m_p / \rho_p)}{(m_p / \rho_p) + (m_{bf} / \rho_{bf})} \quad (14)$$

The mixture of the distilled water and nanoparticles where put in the magnetic stirrer device to be mixed well for one hour in order to ensure the spreading of nanoparticles molecules apart so as not to aggregate quickly. Then the mixture being sent to the ultrasonic cleaner device and kept for 6 hours to mix well. During the experiments, four volume concentrations were used namely, 0.1%, 0.2%, 0.3% and 0.4%, the mass of each concentration calculated from the above relationship .

Table .4 calculation of mass of each concentration added to five liter of distilled water.

| φ% | 0.1% | 0.2% | 0.3% | 0.4% |
|----------|------|------|------|------|
| Mass (g) | 19.2 | 38.4 | 57.6 | 76.8 |

5. Results and Discussion.

5.1.Effect Nanofluid Concentrations and Reynolds number on Frequency of pipe.

Figures. 8, 9,and 10 show the relationship between the frequency of pipe and Reynolds number various with different nanofluid concentrations. It has been shown that the values frequency were increased continuously when Reynolds number increases , more frequency take place at Reynolds number is 130000. For the same Reynolds number the frequency increase as the nanofluid concentration increase, also the ratio of increment increases when the nanofluid concentration increase .This is due to two reasons, firstly that, when Reynolds number values increase this mean, the nanofluid flow rate increase, the velocity of nanofluid increase, the collision between the nanofluid and the pipe wall increase, this lead to the force exerted on pipe wall increase, and secondary that, when the concentration of nanofluid increase ,the viscosity and density of nanofluid increase , Number of nanopartical increase ,this

deals with the collision between the nanofluid and the pipe wall increase. The results closed to many papers such as Pittard *et. al.* [2004].

Figures.11,12,and 13 illustrate the relation between the frequency of pipe and nanofluid concentration with various volume flow rate. It has been shown that the values frequency increase continuously when nanofluid concentrations increase and the ratio of increment increases as the nanofluid concentrations increase. For the same nanofluid concentration the frequency increases as the flow rates increase, also the ratio of increment increases with the flow rates increase. Reasons for behaviour of curves was the same for previous figures. The results closed to many papers such as Pittard *et. al.*[2004].

5.2. Relation between wall shear stress for frequency variation with volume concentration.

Figures.14,15,and 16 demonstrate the relation between wall shear stress with vibration frequency of the pipe converting nanofluid flow for different value of volume concentrations nanofluid. It has been shown that the values frequency increase continuously when wall shear stress increases and the ratio of increment increases as nanofluid concentrations increase. For the same wall shear stress, the frequency values increase as volume concentration increase, also the ratio of increment increases with the volume concentration. It is obvious that the relation is direct proportional, such that the wall shear stress increases with increasing in values the vibration frequency, then its concluded that the effect increasing of vibration frequency lead to increasing the friction factor between the pipe and the wall and thus increasing in pressure drop. From these figures, it can be evaluated several equations between the wall shear stress and frequency for all volume concentration and for the cases without rubber, with rubber thickness was 3mm and with rubber thickness was 6mm, This equation tabulated in table (5).

Table .5 empirical equation between wall shear stress and frequency.

| Case | Volume concentration % | Equations |
|------------------|------------------------|--|
| Without rubber | $\varphi = 0$ | $\tau = -0.328 + 0.00675f - 1.4256 \times 10^{-5}f^2 + 2.8102 \times 10^{-8}f^3$ |
| | $\varphi = 0.1$ | $\tau = -0.432 + 0.0075f - 1.4424 \times 10^{-5}f^2 + 2.8095 \times 10^{-8}f^3$ |
| | $\varphi = 0.2$ | $\tau = -0.522 + 0.0087f - 1.4389 \times 10^{-5}f^2 + 3.228 \times 10^{-8}f^3$ |
| | $\varphi = 0.3$ | $\tau = -0.7625 + 0.01076f - 2.0166 \times 10^{-5}f^2 + 4.029 \times 10^{-8}f^3$ |
| | $\varphi = 0.4$ | $\tau = -0.847 + 0.01235f - 2.3125 \times 10^{-5}f^2 + 4.64 \times 10^{-8}f^3$ |
| With 3 mm rubber | $\varphi = 0$ | $\tau = -0.943 + 0.0116f - 2.627 \times 10^{-5}f^2 + 4.283 \times 10^{-8}f^3$ |
| | $\varphi = 0.1$ | $\tau = -0.838 + 0.0101f - 2.1347 \times 10^{-5}f^2 + 3.622 \times 10^{-8}f^3$ |
| | $\varphi = 0.2$ | $\tau = -0.3962 + 0.0065f - 7.644 \times 10^{-5}f^2 + 3.7011 \times 10^{-8}f^3$ |
| | $\varphi = 0.3$ | $\tau = -0.6347 + 0.0094f - 1.363 \times 10^{-5}f^2 + 4.737 \times 10^{-8}f^3$ |
| | $\varphi = 0.4$ | $\tau = -0.723 + 0.0101f - 1.5443 \times 10^{-5}f^2$ |

| | | |
|------------------|-----------------|--|
| | | $+5.4542 \times 10^{-8} f^3$ |
| With 6 mm rubber | $\varphi = 0$ | $\tau = -0.408 + 0.0101f - 3.22 \times 10^{-5}f^2 + 1.933 \times 10^{-7} f^3$ |
| | $\varphi = 0.1$ | $\tau = 0.190 + 0.0005f - 3.29 \times 10^{-5}f^2 + 1.933 \times 10^{-7} f^3$ |
| | $\varphi = 0.2$ | $\tau = 0.438 + 0.00461f - 6.09 \times 10^{-5}f^2 + 1.3716 \times 10^{-8} f^3$ |
| | $\varphi = 0.3$ | $\tau = 0.723 + 0.0091f - 8.29 \times 10^{-5}f^2 + 1.141 \times 10^{-7} f^3$ |
| | $\varphi = 0.4$ | $\tau = 0.561 + 0.0048f - 6.06 \times 10^{-5}f^2 + 1.497 \times 10^{-7} f^3$ |

Figures.17, and 18 show the relation between vibration shear stress various with volume flow rates of the carbon steel pipe sections and Pyrex glass section converting nanofluid flow. It has been shown that the values of vibration shear stress were decreased continuously when volume flow rate increased. This is due to that ,when the flow rate increase the sub layer near wall increase ,this causes damping to system .The vibration shear stress of carbon steal pipe sections is higher than that of Pyrex pipe ,this is due to the mass was lower than that of carbon steel, the force exerted on pipe was lower ,this deal with the vibration shear stress is lower ,for all section the case without rubber has more vibration shear stress .This is due to , when the thickness of rubber increase the force exerted on pipe is decrease , vibration shear stress decrease ,where the rubber was damping the vibration. While figures.19, and 20 represent the relation between vibration shear stress various with volume concentration for three cases [without rubber, one rubber, and two rubber] of the carbon steel pipe sections and volume flow rate . It has been shown that the values of vibration shear stress were decreased continuously when volume concentration increased. This is due to ,the particles through nanofluid flow absorbed the vibration ,where coursed to breaking the sub layer of nanofluid flow .

7.Conclusion

In this study, the following conclusions has been evaluated the effect of vibration energy lead to increase sub-layer which broken due to the drag force of flow in pipe .Amount of vibration stress τ_{vib} dependent on shear stress τ_{wall} ,when shear stress increase the vibration stress causing increasing in drag force due to the increasing of interface of stream line. Experimental results indicate several empirical equations between shear wall stress and frequency of pipe ,at different flow rates and volume concentrations of nanofluid. Also, using two rubber cases lead to decreasing in fluctuation in pressure values. The frequency of pipe increase as the flow rate and volume concentrations increase.

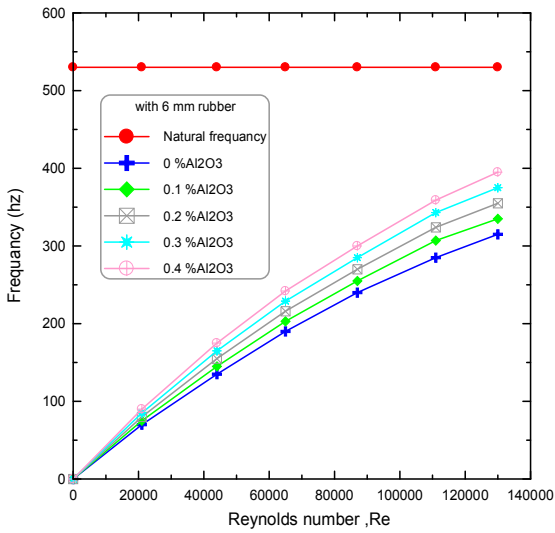


Figure (8) frequency of pipe versus Reynolds number for case with 6 mm rubber .

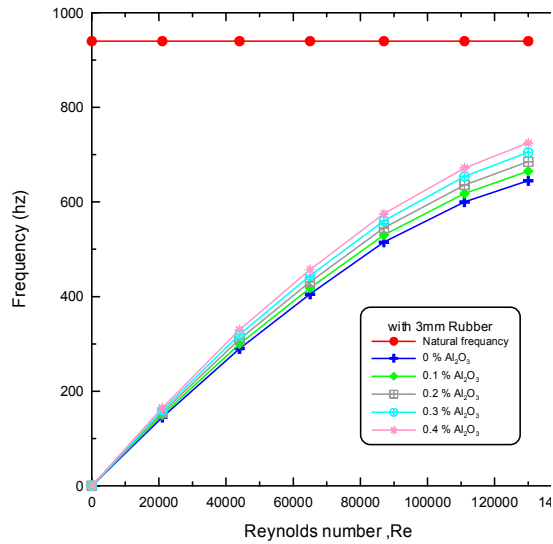


Figure (9) frequency of pipe versus Reynolds number for case with 3 mm rubber

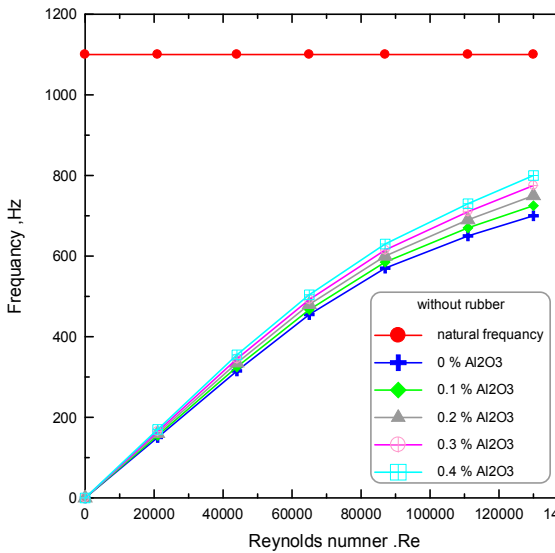


Figure (10) frequency of pipe versus Reynolds number for case without rubber .

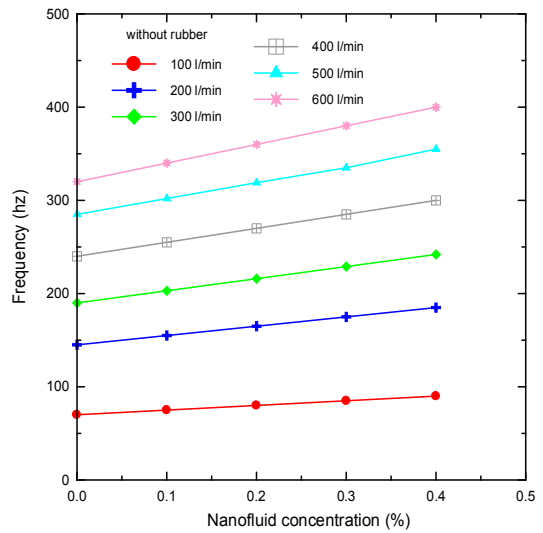


Figure (11) frequency of pipe versus nanofluid concentration for case with 6 mm rubber .

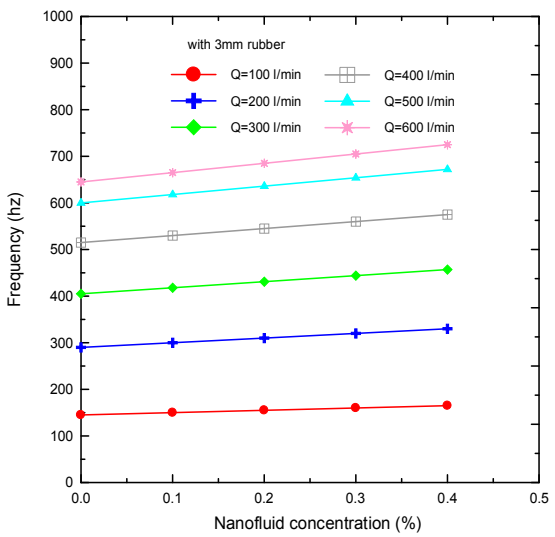
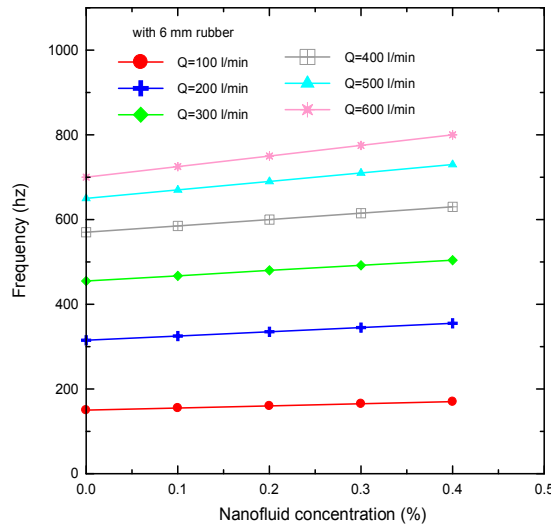


Figure (12) frequency of pipe versus nanofluid concentration for case with 3mm rubber .



Figure(13) frequency of pipe versus nanofluid concentration for case without rubber .

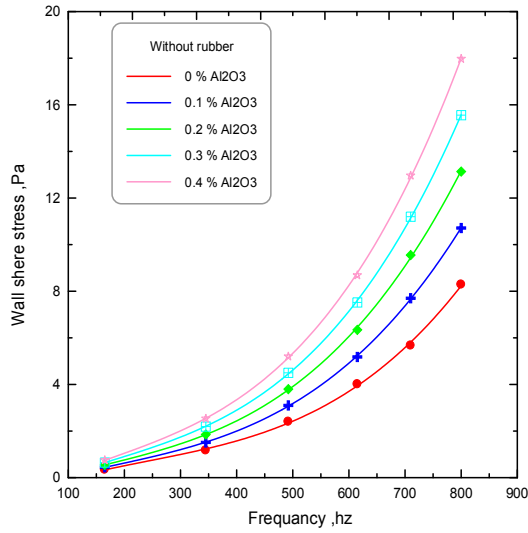


Figure (14) relation between frequency and wall shear stress variation with volume concentrations of nanofluid

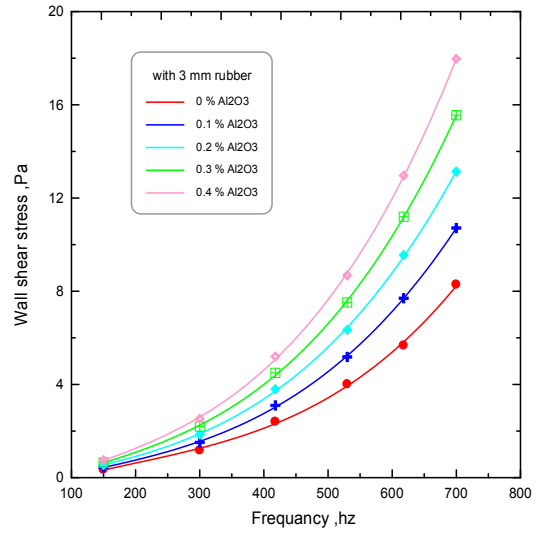


Figure (15) relation between frequency and wall shear stress variation with volume concentrations of nanofluid

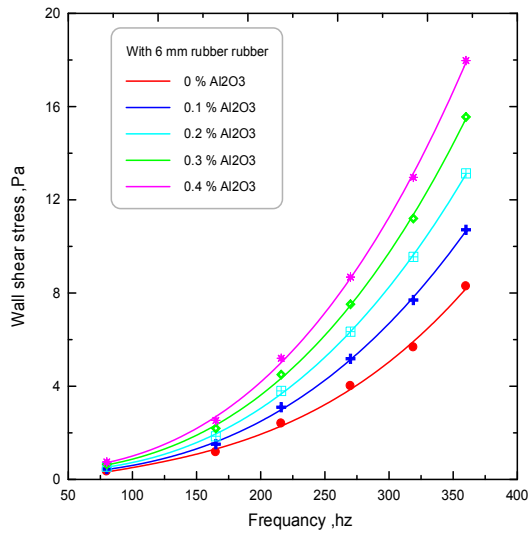


Figure (16) relation between frequency and wall shear stress .

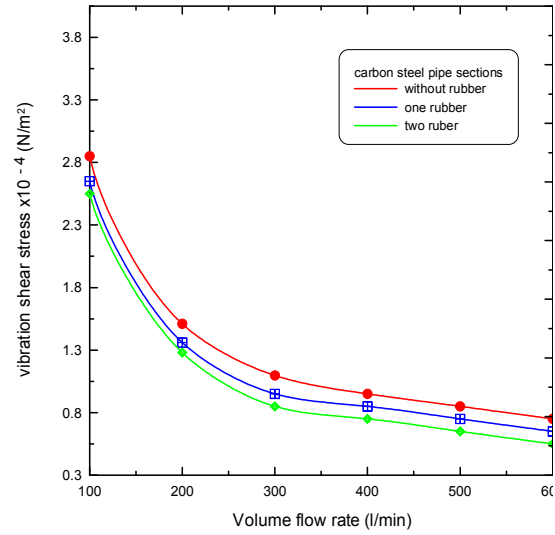


Figure (17) variation vibration shear stress with volume flow rates .

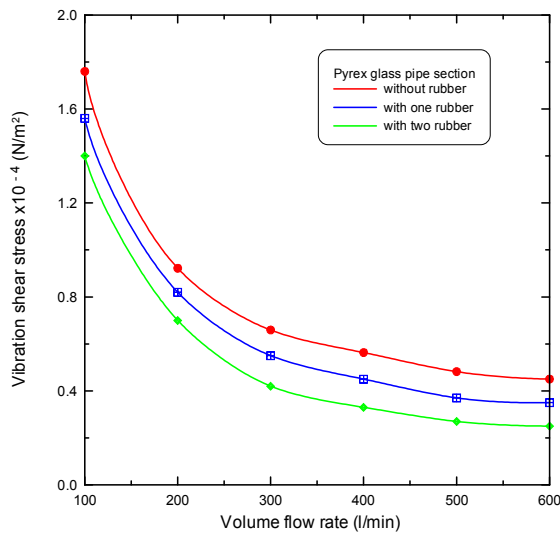


Figure (18) variation vibration shear stress with volume flow rates.

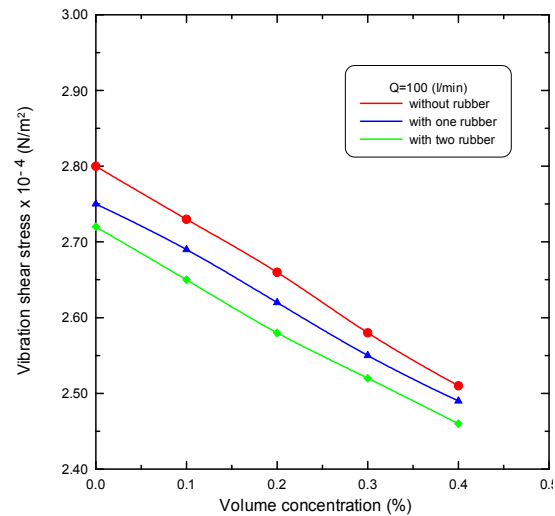


Figure (19) variation vibration shear stress with volume concentrations.

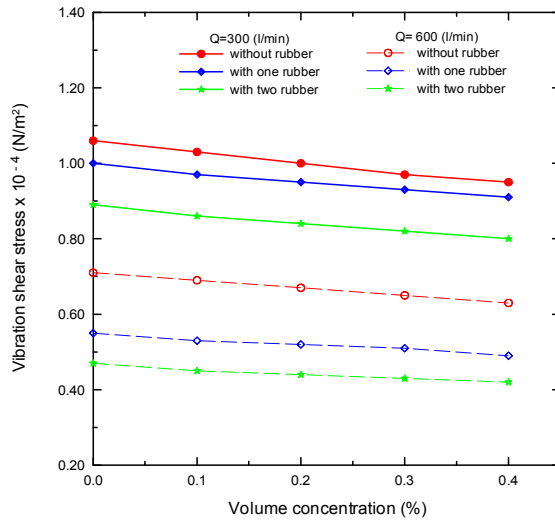


Figure (20) variation vibration shear stress with volume concentrations.

Nomenclature

| Symbol | Descriptions | Units |
|------------|-------------------------------------|-------------------|
| A_a | Acceleration of pipe | m/s ² |
| A_s | Surface area | m ² |
| d_o | Outer diameter of pipe | m |
| d_i | Inner diameter of pipe | m |
| F | Force | N |
| f_w | Frequency of pipe with nanofluid | Hertz |
| f_d | Frequency of pipe without nanofluid | Hertz |
| f | Frequency of pipe | Hertz |
| m | mass | gram |
| p | Pressure | N/m ² |
| Δp | Pressure drop | N/m ² |
| P_o | power | W |
| Re | Reynolds number | --- |
| r | Radius of pipe | m |
| u | Velocity in z-direction | m/s |
| V_a | Velocity of pipe | m/s |
| V_{nf} | Volume of nanofluid | m ³ |
| V | Volume flow rate | m ³ /s |
| y | Amplitude of pipe | m |

| Greek Symbols | | |
|---------------|--------------------------------|-------------------|
| ϕ | Particles volume concentration | % |
| ρ | Density | kg/m ³ |
| ξ | Damping ratio | ---- |
| τ_{nf} | Shear stress | N/m ² |
| τ_{vib} | Vibration shear stress | N/m ² |

References

- Adekunle O. Adelaja, 2013**, "Temperature modulation of the vibrational responses of a flexible fluid-conveying pipe" Central European Journal of Engineering December 2013, Volume 3, Issue 4, pp 740-749 .
- Bagchi K., Gupta S.K., Kushari A. and Iyengar N.G.R., 2009**, "Experimental Study of Pressure Fluctuations and Flow Perturbations in Air Flow Through Vibrating Pipes," Journal of Sound and Vibration 328 pp. 441–455.
- Birgersson F., Finnveden S., and Robert G., 2004**, "Modelling Turbulence- Induced Vibration of Pipes with a Spectral Finite Element Method" ,Journal of Sound and Vibration Vol.27, pp.749-772,.
- Blevins R. D., 1977**, Flow Induced Vibrations. Book, Van Nostrand Reinhold Ltd, New York,.
- Chang J.S. and Chiou W.J., 1995**, "Natural Frequencies and Critical Velocities of Fixed-Fixed Laminated Circular Cylindrical Shells Conveying Fluid", Journal of Computers and Structures, Vol.57, No.5, pp.929-939.
- Francis, 1983**, "Mechanical Vibration, Theory and Application", 3rd Edition, Addison-Wesley, USA,.
- Fotukian M., and Esfahany N., 2010**, "Experimental investigation of turbulent convective heat transfer of dilute γ -Al₂O₃/water nanofluid inside a circular tube" International Journal of Heat and Fluid Flow .Vol.31 , pp.606–612 .
- Holman J. P., 2010**, "Heat Transfer" book Tenth Edition, Published by McGraw-Hill, USA .
- Jeong W.B., Seo, Y.S., Jeong S.H., Lee S.H., and Yoo, W.S., 2006**, "Stability Analysis of a Pipe Conveying Periodically Pulsating Fluid Using Finite Element Method", JSME International Journal, Series C, Vol. 49, pp.1116-1122.
- Kohli A. K. and Nakra B.C., 1984**, "Vibration Analysis of Straight and Curved Tubes Conveying Fluid by Means of Straight Beam Finite Elements," Journal of Sound and Journal Vibration, Vol.93, No.2, pp.307-311.
- Matthew T. Pittard and Robert P. Evans and R. Daniel Maynes , 2004**, "Experimental and numerical investigation of turbulent flow induced pipe vibration in fully developed flow" AIP Journal. Vol. 75, Number 7.
- Paidoussis M.P. , and Issid N.T., 1994**, "Dynamic stability of pipes conveying fluid" Journal of Sound and Vibration Volume 33, Issue 3, 8 April 1974, pp.267–294.
- Pak, B.C., Cho, Y.I., 1998**, "Hydrodynamic and Heat Transfer Study of Dispersed Fluids with Submicron Metallic Oxide Particles" Journal of experimental heat transfer, Vol.11 ,pp.151-171.
- Raja M., Arunachalam R.M., and Suresh S., 2012**, "Experimental studies on heat transfer of alumina/water Nanofluid in a shell and tube heat exchanger with wire coil " International Journal of Mechanical and Materials Engineering (IJMME), Vol. 7, pp.16–23.
- Wang L., Dai H. L., 2012**, "Vibration and enhanced stability properties of fluid-conveying pipes with two symmetric elbows fitted at downstream end " Archive of Applied Mechanics February, Volume 82, Issue 2, pp 155-161.
- Willatzen M., 2003**, "Liquid flows and vibration characteristics of straight-tube cylindrical shells "Journal of Sound and Vibration Volume 260, Issue 3, 20 February 2003, pp. 417– 429.
- Wijdan .K Sahib, 2013**, " , Effect of design conditions on vibration in pipr conveying fluid " A THESIS Submitted to the College of Engineering University of Baghdad in Doctor of philosophy in Mechanical Engineering January.
- Yih-Hwang Lin, and Yau-Kun Tsai , 1997**, " Nonlinear vibrations of Timoshenko pipes conveying fluid "International Journal of Solids and Structures Volume 34, Issue 23, pp. 2945–2956 .